Cygnus 2013
Toyama, Japan
10-12 June 2013

Energy partition and distribution of excited species in direction-sensitive detectors for WIMP searches

Akira Hitachi **Kochi Medical School**

Key words:
$S_T = S_e + S_n$
quenching factor $q_{nc} = \eta/E$
$LET_{el} = d\eta/dx$
Bragg-like curve: $d\eta/dR_{PRJ}$

Don't miss ISON in late this year

PANSTARRS c/2011 L4

Head–tail discrimination

The Bragg-like curve for head-tail detection

The distribution of the electronic energy η deposited in the detector gas as a function of the ion depth, i.e. projected range R_{PRJ}.

$\Delta\eta/\Delta R_{PRJ}$

It is an averaged one dimensional presentation. For slow ions, it is not given by the electronic stopping power, $S_e = (dE/dx)_e$.
One needs the Lindhard factor $q_{nc} = \eta/E$.

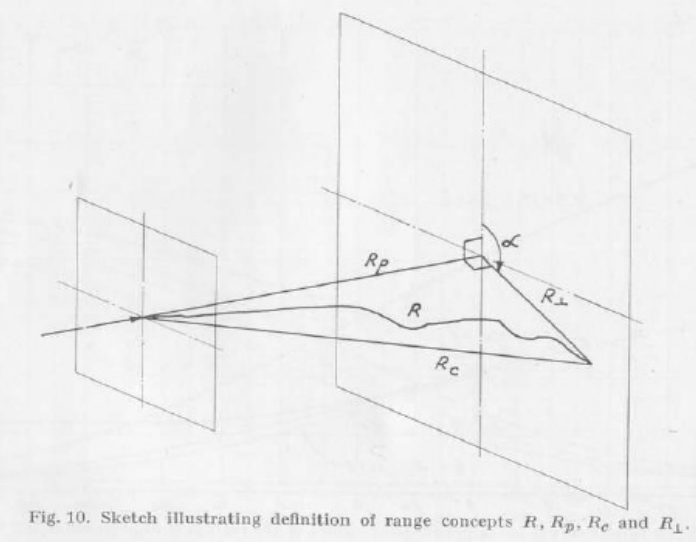

Fig. 10. Sketch illustrating definition of range concepts R, R_p, R_c and $R_\perp$.

Nuclear Stopping Power

Interaction potential

$$U(r) = (Z_1 Z_2 e^2 / r) \cdot \phi(r/a)$$

$\phi(r/a)$: Fermi function

$$a = 0.8853 \cdot a_0 \left(Z_1^{2/3} + Z_2^{2/3}\right)^{-1/2}$$

A universal differential cross section

$$d\sigma = \pi a^2 \frac{dt}{2t^{3/2}} f(t^{1/2})$$

$$t = \varepsilon^2 \cdot (T/T_m) = \varepsilon^2 \sin^2 \frac{\theta}{2}$$

The nuclear stopping power

$$\left(\frac{d\varepsilon}{d\rho}\right)_n = \int_0^{\varepsilon} dx \frac{f(x)}{\varepsilon}$$

A screened Rutherford scattering

[⇒ exp(-r/a_B): Bohr]

a: Thomas-Fermi type screening radius

$f(t^{1/2})$

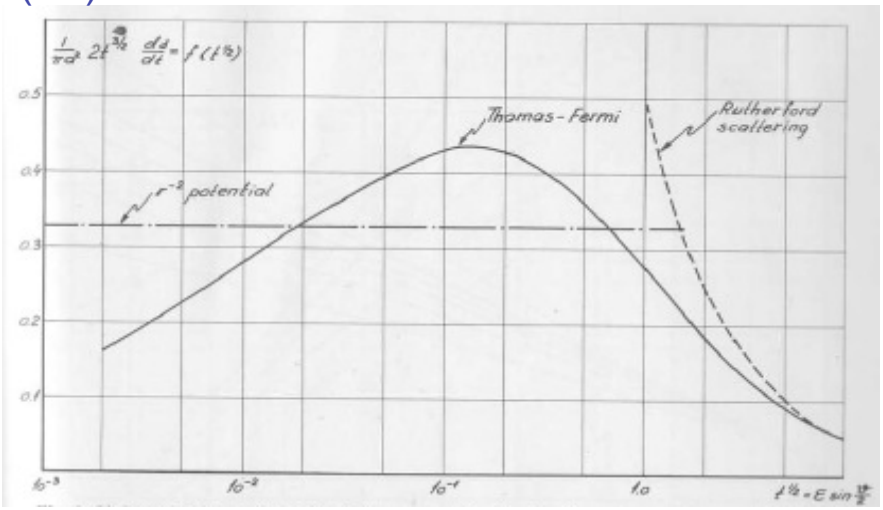

$t^{1/2} = \varepsilon \sin(\theta/2)$

Stopping Powers

The nuclear stopping power S_n

$$S_n(E) = \frac{< T(E) >}{\lambda(E)} = N\sigma < T >= N\sigma \int_0^\infty T(E,\theta(p)) \frac{2\pi p dp}{\sigma} = \pi N \int_0^\infty T d(p^2)$$

$<T(E)>$ is the mean energy transferred in an elastic collision, and $\lambda(E) = 1/N\sigma$

$$T(E,\theta) = \frac{4A_1A_2}{(A_1+A_2)^2} E \sin^2 \frac{\theta}{2}$$

S_n can be expressed by the analytical expression [Birsack 1968]

$$S_n = -\frac{dE}{ds} = \frac{4\pi a N A_1 Z_1 Z_2 e^2}{A_1 + A_2} \cdot \frac{\ln \varepsilon}{2\varepsilon(1-\varepsilon^{-3/2})}$$

for all Z_1, Z_2

The electronic stopping power S_e

An atom moving though an electron gas of constant density. Using a Thomas-Fermi treatment, [Lindhard & Scharff]

$$S_e = \xi_e \times 8\pi e^2 a_0 \cdot \frac{Z_1 Z_2}{(Z_1^{2/3} + Z_2^{2/3})^{3/2}} \cdot \frac{v}{v_0}$$

$$\xi_e \approx Z_1^{1/6}$$

for all Z_1, Z_2

$S_e = k\varepsilon^{1/2}$: 0.1 ～ 0.2

Stopping Power Lindhard

Low energy

$v < v_0 = e^2/\hbar$

The generalized range and energy

$$\rho = RNA_2 \cdot 4\pi a^2 \frac{A_1}{(A_1 + A_2)^2}$$

$$\varepsilon = E \frac{aA_2}{Z_1 Z_2 e^2 (A_1 + A_2)}$$

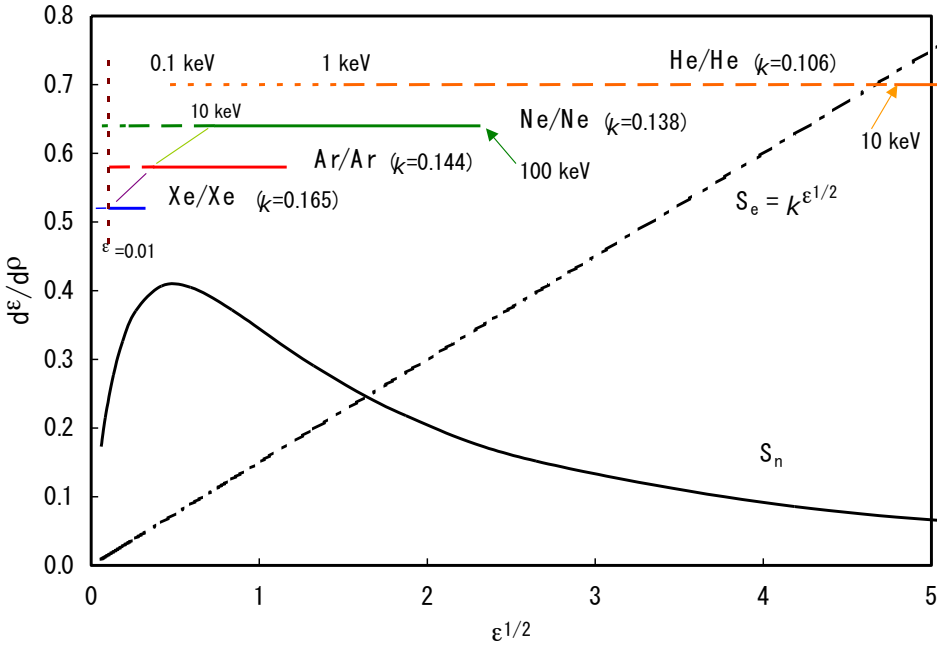

Nuclear S_n and electronic S_e stopping powers as a function of energy ε for k=0.15.

The Thomas-Fermi treatment becomes a crude approximation at the extreme low energy and separation of the nuclear scattering and electronic stopping becomes uncertain. LSS theory is not very reliable at $\varepsilon < 0.01$, i.e., below 10 keV for Xe ions in Xe.

In this sense, almost all the stopping theory available is not reliable below $\varepsilon < 0.01$.

Lindhard factor $q_{nc} = \eta/\varepsilon$

The stopping powers contain only a part of the necessary information to obtain the quenching factor, $q_{nc} = \eta/\varepsilon$ ratio. The differential cross section in nuclear collisions is needed for the integral equations. For $Z_1 = Z_2$,

$$\left(\frac{d\varepsilon}{d\rho}\right)_e \cdot \nu'(\varepsilon) = \int_0^{\varepsilon^2} \frac{dt}{2t^{3/2}} \cdot f(t^{1/2}) \left\{ \nu\left(\varepsilon - \frac{t}{\varepsilon}\right) - \nu(\varepsilon) + \nu\left(\frac{t}{\varepsilon}\right) \right\}$$

$$\left(\frac{d\varepsilon}{d\rho}\right)_e = k\varepsilon^{1/2}$$

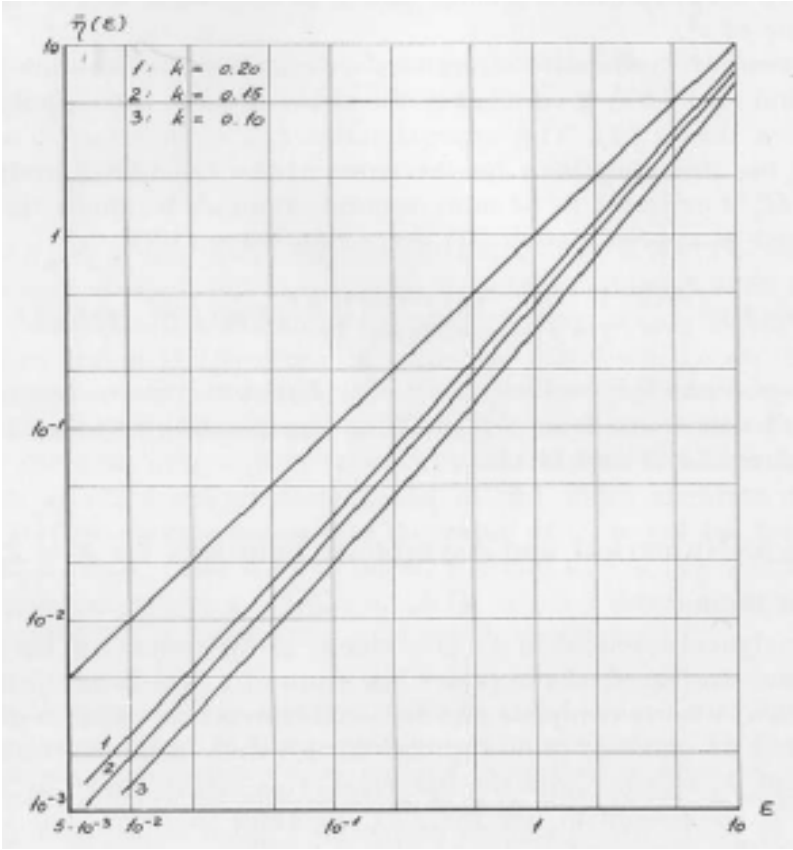

η as a fn of ε for k = 0.2, 0.15, 0.1

$\varepsilon = \eta + \nu$

Electronic Linear Energy Transfer (LET_{el})

$LET_{el} \equiv -d\eta/dR = -\Delta\eta/\Delta R$ R: the range

$= -(\eta_1-\eta_0)/(R_1-R_0)$

for quenching calc. etc.

The true range R is given by the total stopping power

$$R_T = \int (dE/dx)_{total}^{-1}\, dE$$

The Bragg-like curve for TPC

The projected range, R_{PRJ}, may be used

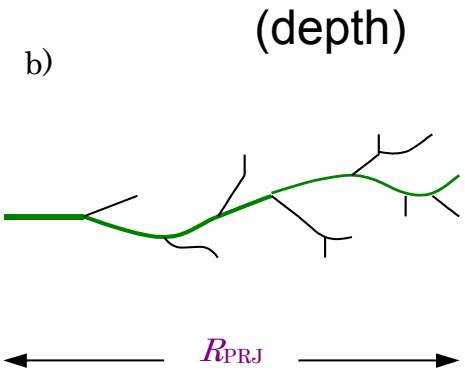

Birks' eq.

$$\frac{dL}{dx} = \frac{C_1(-dE/dx)}{1 + C_2(-dE/dx)}$$

LET_{el} should be used, not S_{el} .

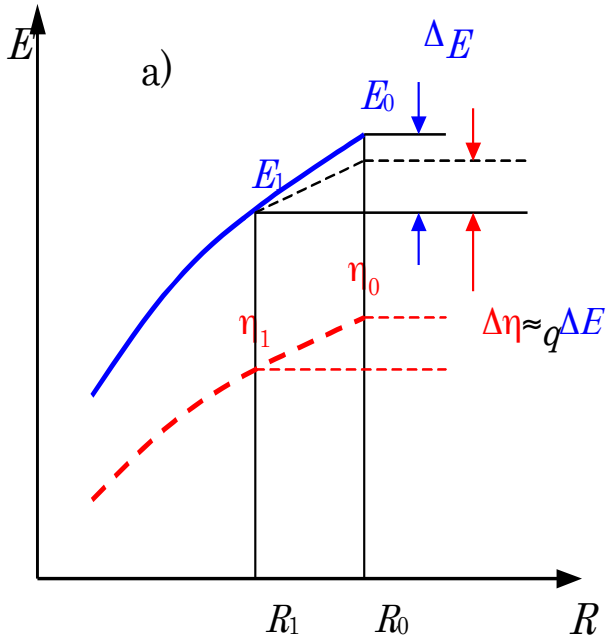

Stopping Power and LET

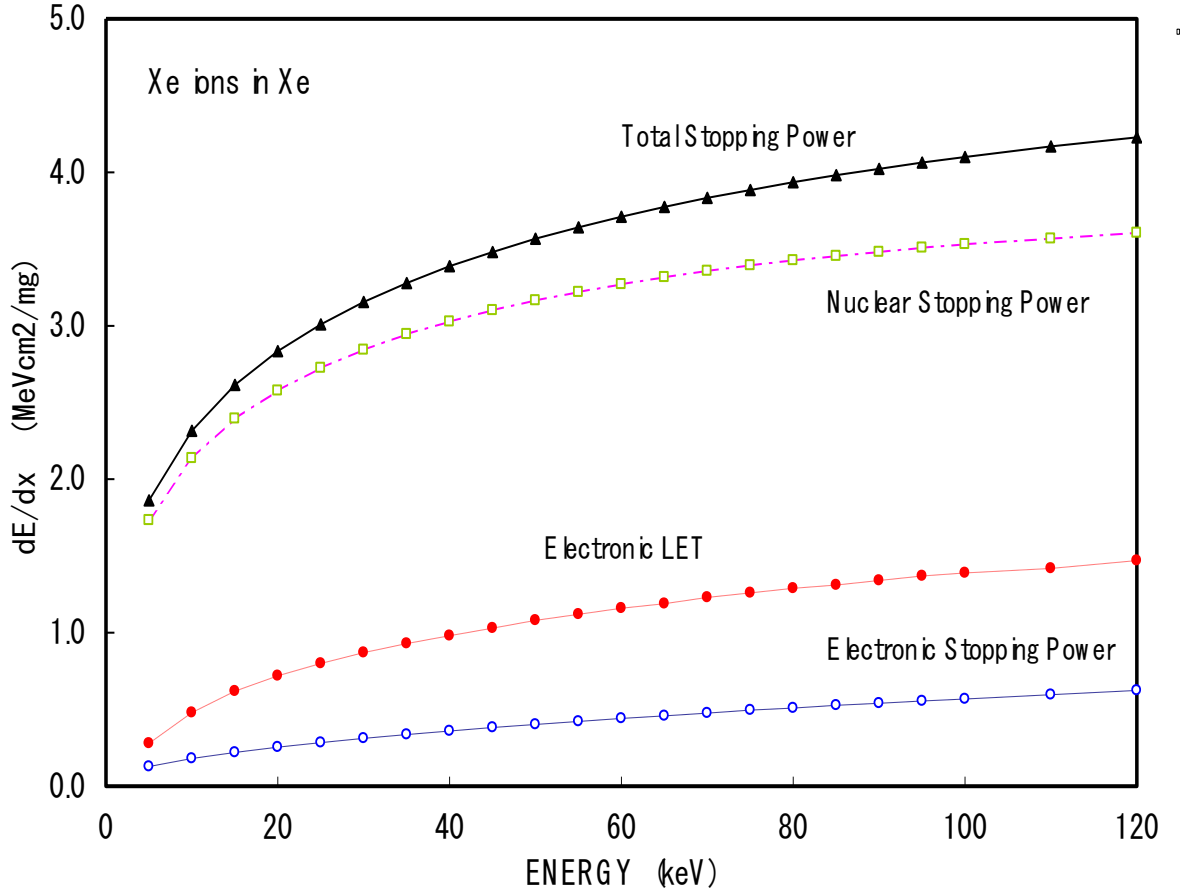

Fig. 1 The stopping power and the electronic LET as a function of the recoil energy for Xe in Xe.

HMI & Lindhard

Bragg-like curve

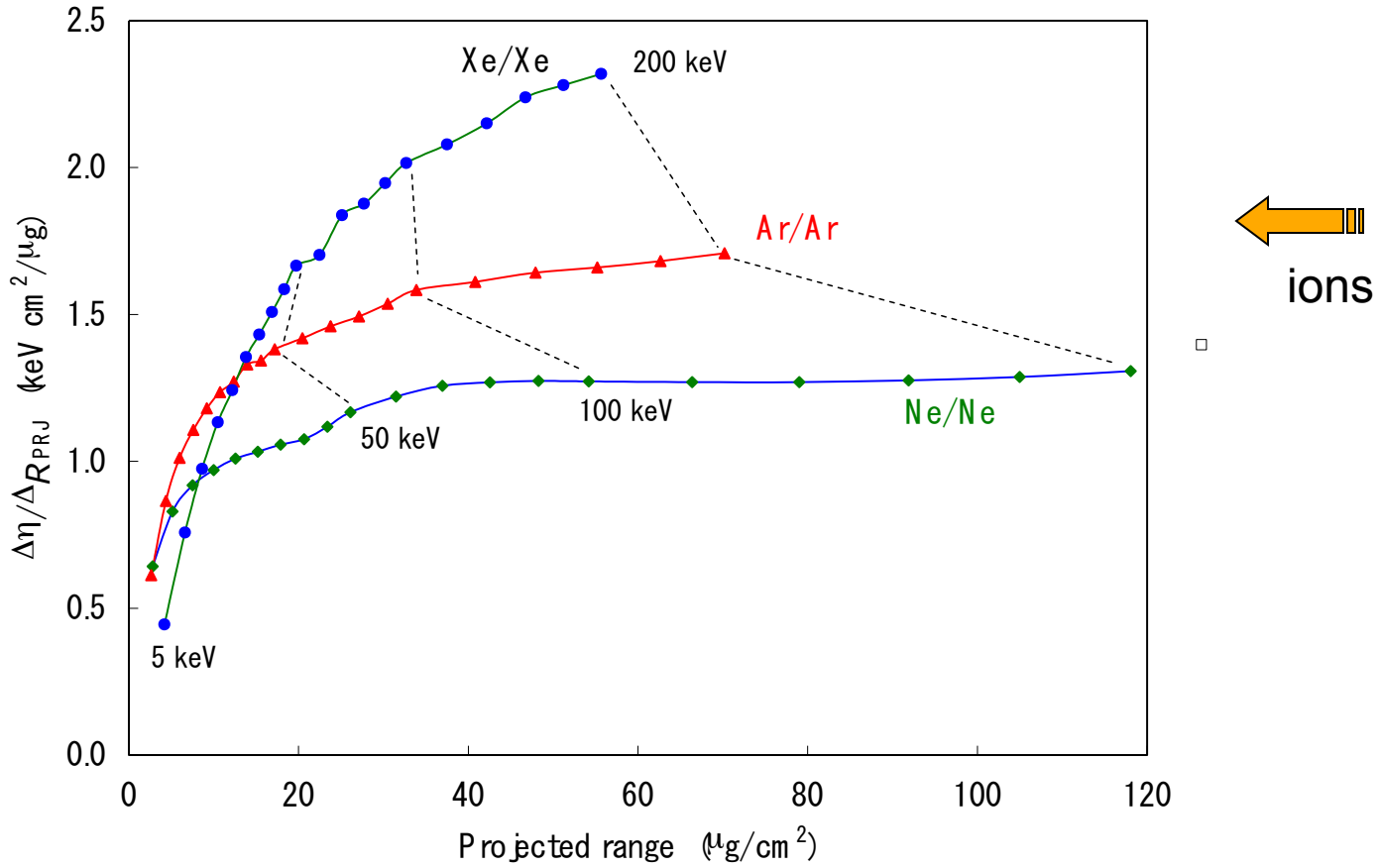

Bragg-like curves, $d\eta/dR_{PRJ}$ for recoil ions in rare gases.

The ions enter from the right hand side. Points are plotted at every 5, 10 or 20 keV

The projected ranges are taken from SRIM.

Head and tail detection of WIMPs

He in He (+5%C_4H_{10})

Ionizing particle produces excited atoms He* and ions He^+.

Then formation of excited molecules,

$$He^* + He + He \rightarrow He_2^* + He$$

molecular ions,

$$He^+ + He + He \rightarrow He_2^+ + He$$

and higher excited states

$$He^+ + e^- + He \rightarrow He_2^* + He$$

Hornbeck-Molnar Process

$$He^*(n \geq 2) + He \rightarrow He_2^- + e^-$$

Penning ionization

$$He^* + M \rightarrow He + M^+ + e^-$$

$$He_2^* + M \rightarrow He + He + M^+ + e^-$$

There are passes to no ionization

He* + M → He + M(excitation, dissociation, non radiative decay)

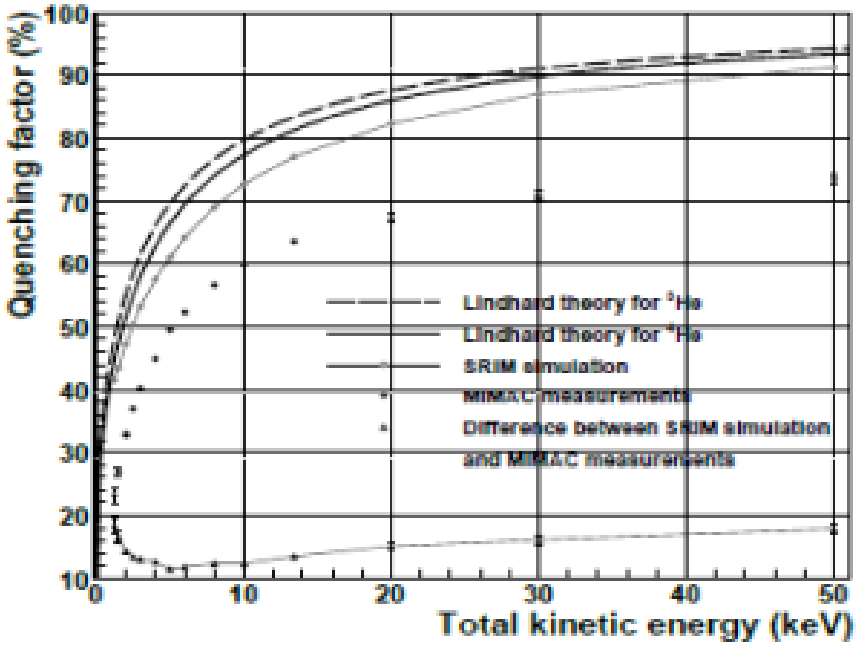

He in He+5%C_4H_{10} Santos 2008

The measured points are considerably smaller than Lindhard and SRIM.

The W-value can depend on He pressure and dopant pressure.

W-value

The energy balance of absorbed energy T and W value:

$$T_0 = N_i/\bar{E}_i + N_{ex}/\overline{E_{ex}} + N_i\bar{\varepsilon}$$

$$W = T_0/N_i = \bar{E}_i + \overline{E_{ex}}(N_{ex}/N_i) + \bar{\varepsilon}$$

$W_\alpha/W_\beta \approx 1$ for rare gases
fast ions

Contributions of 2^1S and 2^3S may be added for slow ions in He.

He(2^1S) , He(2^3S) and $He_2(2^1S)$ and $He_2(2^3S)$ are 'true' metastables.
He(2^1S) and He(2^3S) were not produced directly by fast particles; however can be produced directly by slow ions.

Resonance trapping for He(2^1P). (low pressure)

A part of energy will diffused out of the chamber.

The W-value can depend on energy and type of the incident particle at low energy.

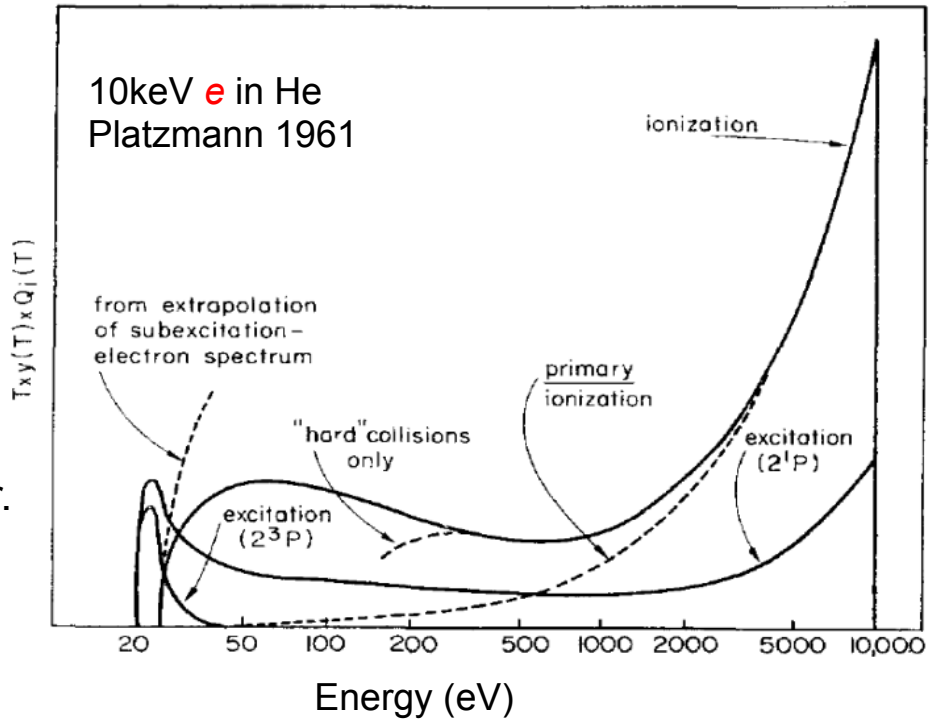

Contribution to ionization and excitation.

Lindhard factor for $Z_1 \neq Z_2$

The formation of accurate general solutions become quite complicated. The integral equation for the ion Z_1 in the matter Z_2 is,

$$\nu_1'(E)\cdot S_{1e} = \int d\sigma_1 \{\nu_1(E-T) - \nu_1(E) + \nu(T)\}$$

$d\sigma_1$: the diff. cross section for an elastic colli. between Z_1 and Z_2.

$T < T_m = \gamma E$; $\gamma = 4A_1A_2/(A_1+A_2)^2$

Characteristic energies:

$E_{1c} \cong A_1^3(A_1+A_2)^{-2}Z^{4/3}Z_1^{-1/3}\cdot 500$ eV, $E_{2c} \cong (A_1+A_2)^2 A_1^{-1}Z_2 \cdot 125$ eV, where $Z^{2/3} = Z_1^{2/3} + Z_2^{2/3}$

The power law approximation for very low energy,

$$\eta = CE^{3/2} \qquad C = \frac{2}{3}\left\{E_{1c}^{-1/2} + \frac{1}{2}\gamma^{1/2}E_c^{-1/2}\right\},$$

for $E < E_{1c}$, E_{2c},

The straggling:

$$\Omega^2/\eta^2 = \frac{1}{14}\gamma\left\{\left(\frac{\gamma^{1/2}}{CE_c^{1/2}} - \frac{7}{4}\right) + \frac{7}{16}\right\}$$

Good for heavy ions such as Pb ions in α−decay

Lindhard factor for recoil ions in α-decay

Recoil ion	206Pb		208Tl		208Pb		*E*2c
Energy keV	103		117		168		
gas	expt	calc	expt	calc	expt	calc	keV
Ar	0.221a	0.196	0.263	0.205	0.294	0.249	665
Xe	0.139 a	0.124		0.132		0.158	3730
H2		0.73	0.457	0.78	0.544	0.93	26
He		0.53	0.500b	0.56	0.546 b	0.68	53
CH4	0.250		0.265		0.307		
C2H4	0.236		0.269		0.321		
C3H6			0.272		0.281		
CO2			0.336		0.347		
C + 2O		0.297		0.316		0.378	174
C		0.323		0.344		0.411	174
O		0.284		0.302		0.361	241
N2	0.319	0.302		0.320		0.384	207
Dry air	0.296						
4N + O		0.298		0.317		0.379	207
CS2							
C + 2S		0.246		0.262		0.314	174
S	0.208						550
Al (for CS2)	0.228						428

Recoil ion		214Pb		210Pb			
Energy keV		112	calc	147	calc		
CS2			0.346		0.397	SRIM by P.J.	
C + 2S			0.253		0.292		174
Al (for CS2)			0.237		0.272		430

calc : the power law approximation by Lindhard which is only good at E<E2c.

expt : W(alpha)/W(recoil) from:

[a] G.L.Cano, Phys. Rev. 169, 227 (1968). [b] W.G. Stone & L.W. Cochran, Phys. Rev. 107, 702 (1957).

Binary gases

Binary gases such as CS_2 , CF_4

S_T the Bragg rule

compound correction

Simple approximation for q_{nc}

to consider only one element at a time.

C in CS_2 ⇒ C in C,

S in CS_2 ⇒ S in S

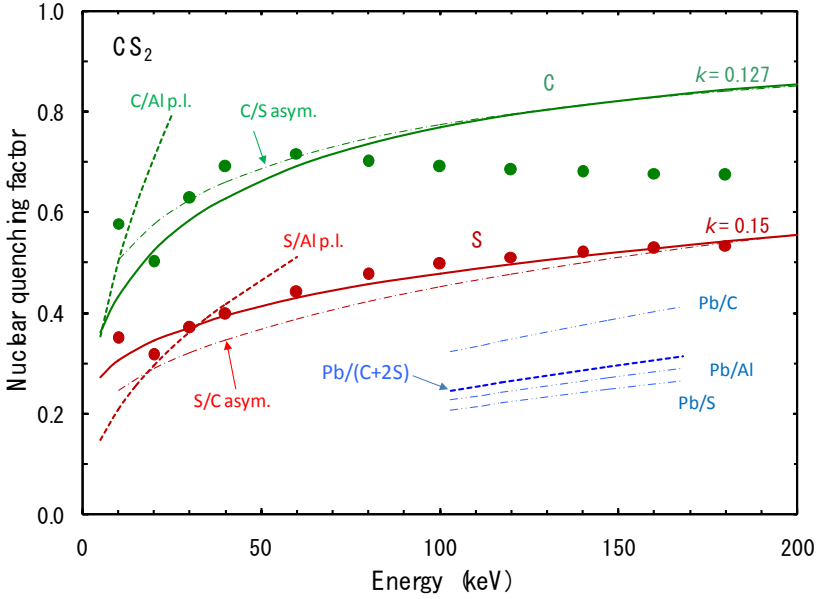

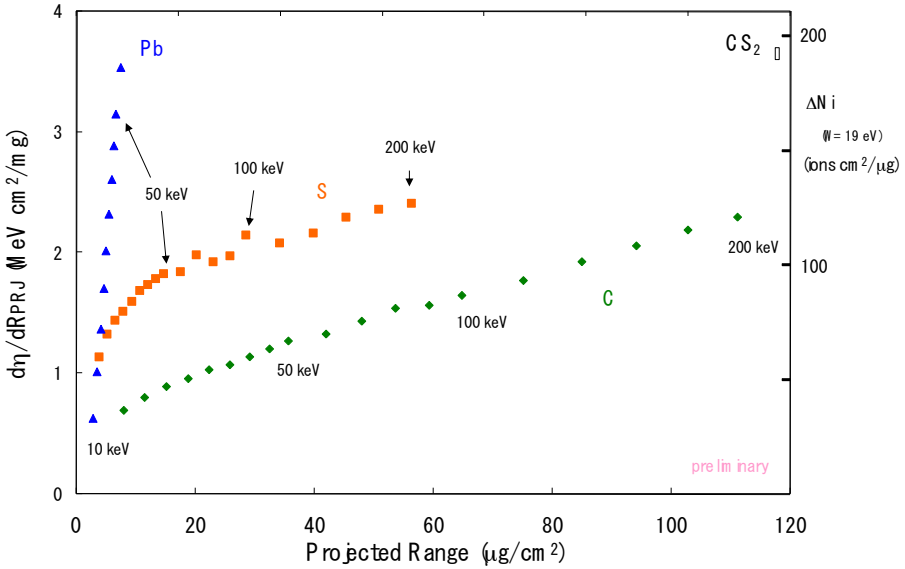

solid : C ions in C, S ions in S

dashed : Asymptotic eq. C and S in Al

●,● : Snowdon-Ifft expt.

Power law approximation

1/3(Pb in C)+2/3(Pb in S)

CF_4

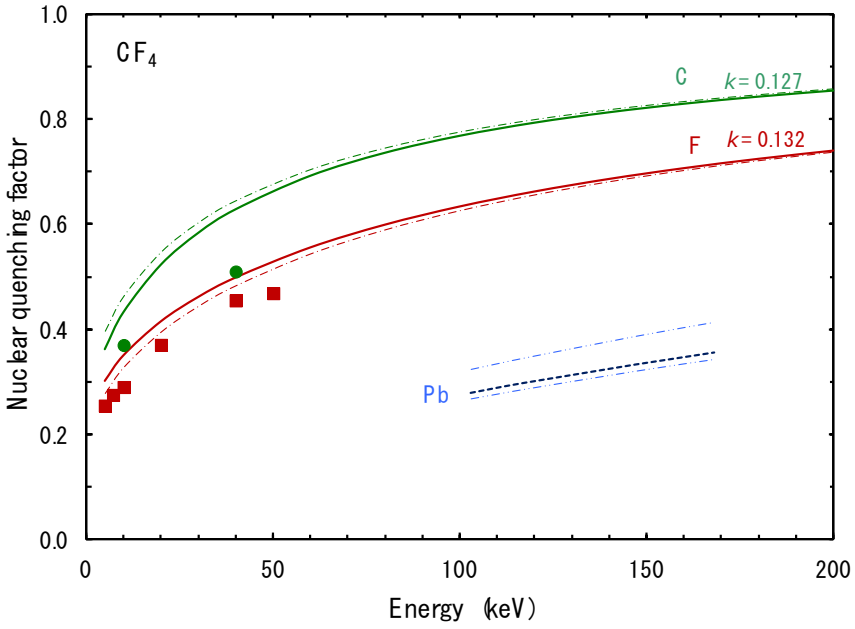
CF4
C
k= 0.127
F
k= 0.132
Pb
Nuclear quenching factor
Energy (keV)
0.0
0.2
0.4
0.6
0.8
1.0
0
50
100
150
200

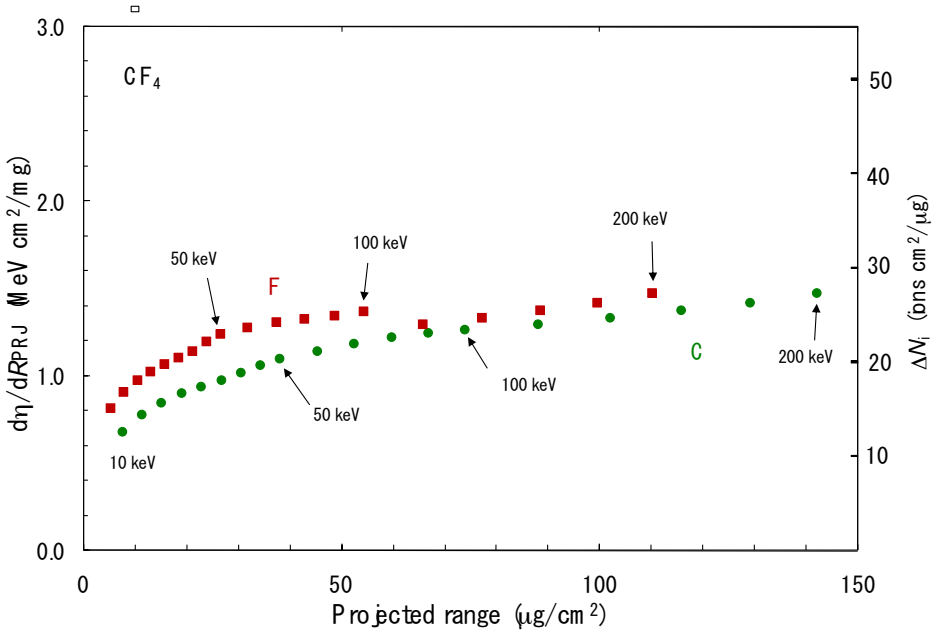
CF4
50 keV
100 keV
200 keV
F
C
10 keV
50 keV
100 keV
200 keV
dη/dRPRJ (MeV cm2/mg)
ΔNi (ions cm2/μg)
Projected range (μg/cm2)
0.0
1.0
2.0
3.0
10
20
30
40
50
0
50
100
150

[C]:[F] = 1:4

fast ions

The maximum impact parameter b_{max} is given by Bohr's impulse principle

$$b_{\max} = \hbar v / 2E_1$$

v: the incident ion velocity

$\hbar$: Planck's constant divided by 2π

E_1 : the lowest excitation energy.

Excitation by the light ions (p, α) described theoretically in terms of perturbation by an incident point charge.

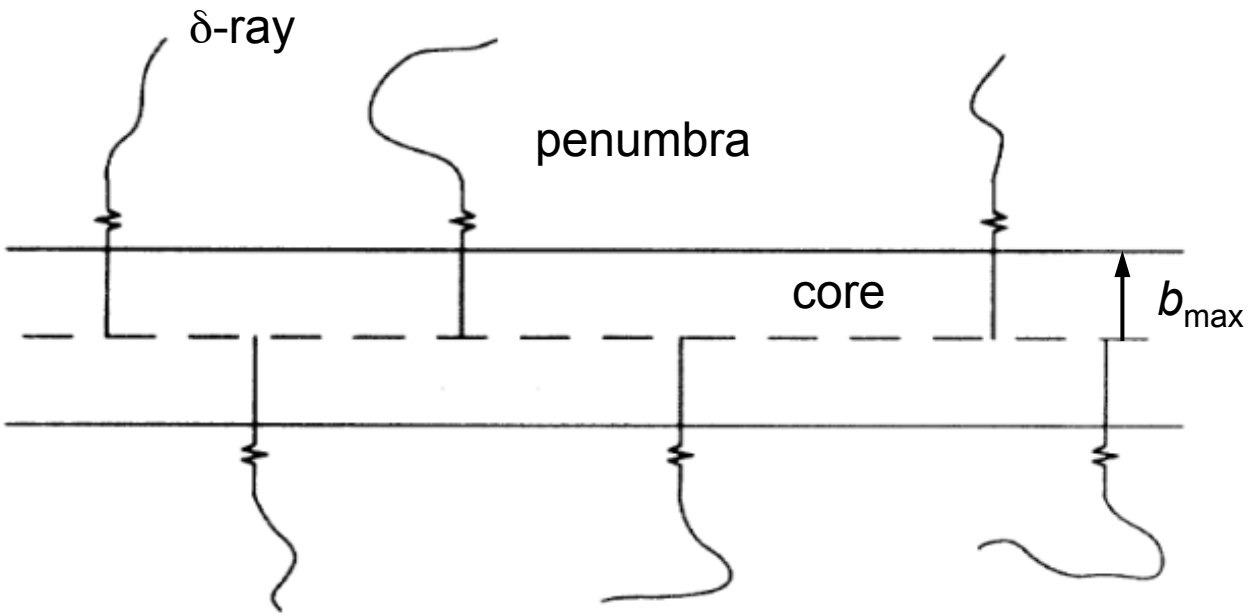

Stopping power for slow light particles

The Coulomb effect
the deflection and deceleration of the projectile in the field of the nucleus.

The Threshold effect
the energy delivered to e^- must be as large as *I*.

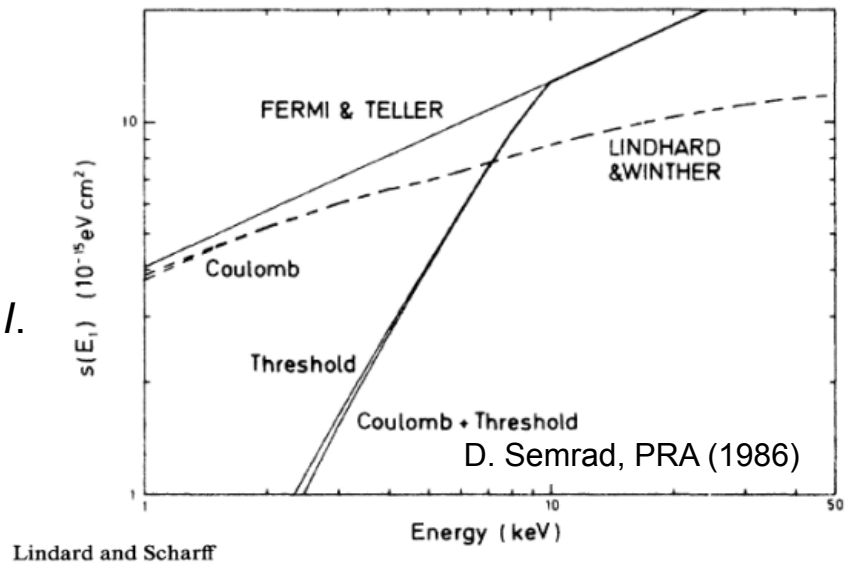

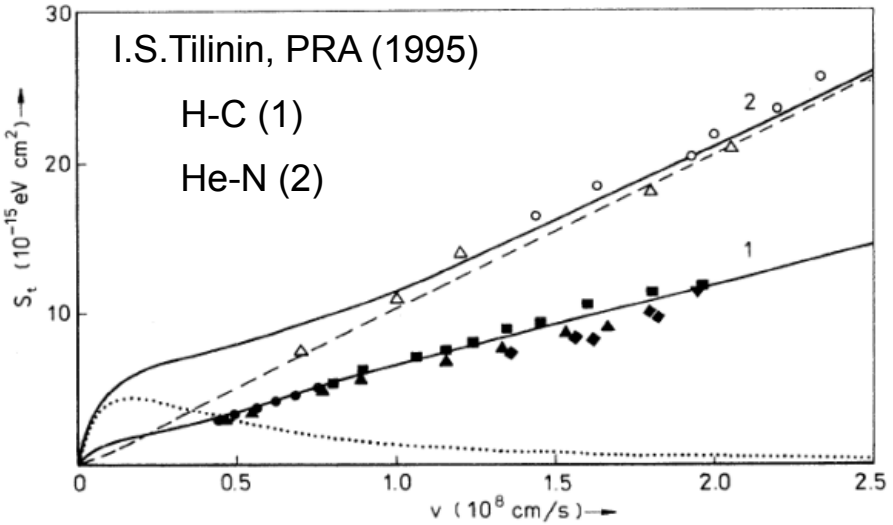

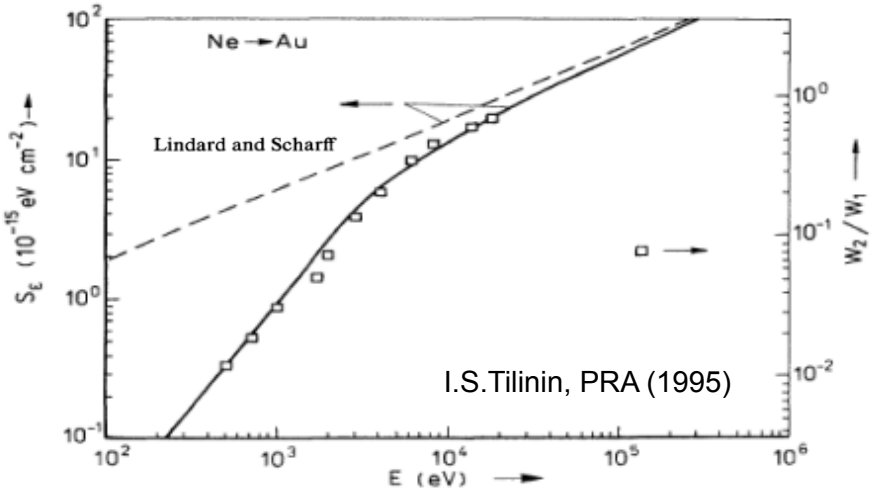

SRIM or TRIM

Based on The B-K theory originally TRIM was for light particles and at high energy.
It adapted the LSS theory for slow heavy ions.

as the degree of ion stripping. Also, calculations are made from fundamental theories like the Brandt–Kitagawa theory and LSS theory [18]. If the experimental values are within reasonable agreement with this set of theoretical calculations, then the experimental values are weighted with the theoretical values to obtain final values.

SRIM, NIMB 2012

The measurement of stopping power for heavy ions of low velocity is quite difficult
Usually, $S_T = S_e + S_n$ is measured and often Lindhard is assumed for S_e.

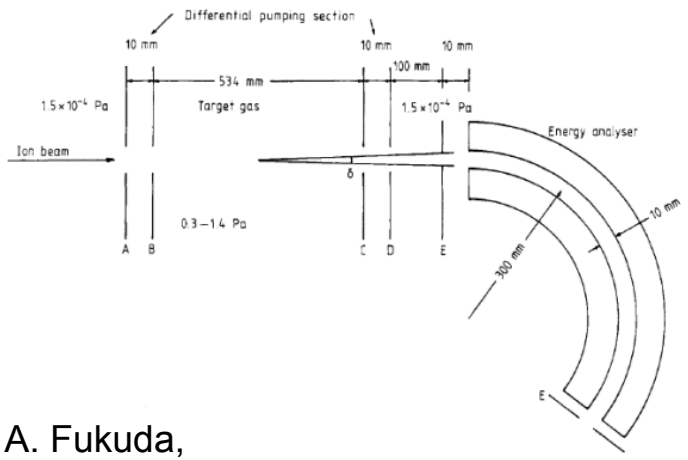

A. Fukuda,

J. Phys. B: At. Mol. Phys. **14** (1981) 4533.

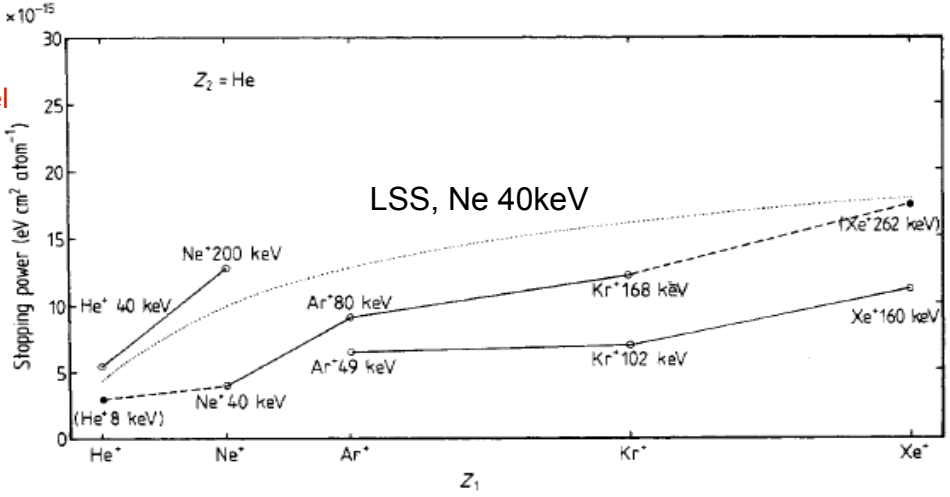

Figure 8. Z_1 dependence of He stopping powers. The points of the same velocity are connected by straight lines. The dotted curve shows the theoretical values for LSS theory for the velocity of Ne^+ of 40 keV.

The spectrometer determines the energy quite accurately; however, the measurement does not take contribution from $\theta > 0$.

Heavy-particle collisions at low energy

When atomic projectile goes hard (wide deflection angle small impact parameter) collision with atom, the large inelastic energy losses occur at characteristic internuclear distances. Showers of fast-electrons are thrown out.

Inelastic energy losses Q for Ar^+-Ar collision

T_0,θ	m,n	$\bar{Q}_{mn}$ (eV)	m,n	$\bar{Q}_{mn}$ (eV)
6 keV, 8°	T,T	57±3	1,1	55±3
	0,1	36±3	2,1	79±4
	1,0	30±4		
25 keV, 16°	T,T^a	90±17	$2,2^b$	353±7
	T,T^b	379±10	$2,3^b$	362±9
	T,T^c	613±14	$2,3^c$	636±14
	$1,1^a$	62±6	$3,3^b$	468±6
	$2,2^a$	160±7	$3,3^c$	647±10

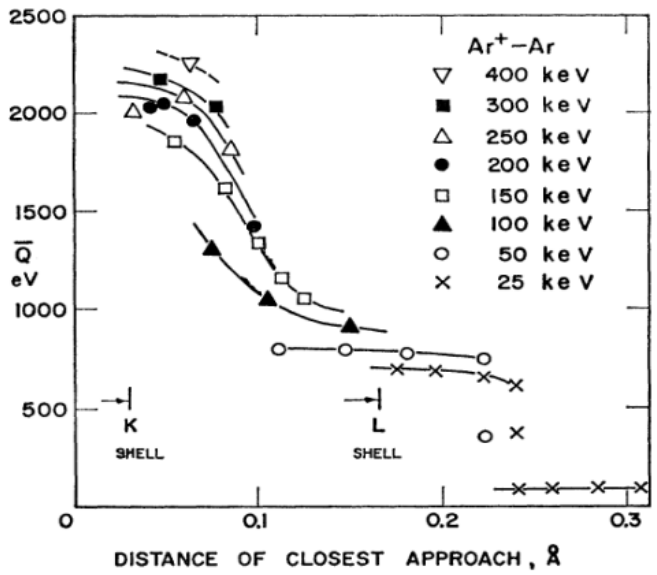

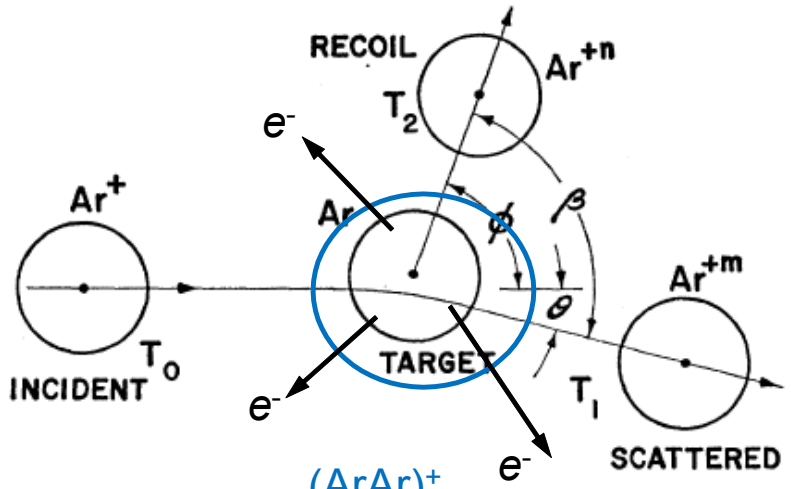

$(ArAr)^+$
Molecular Orbit (MO)

Kessel & Everhart, PR146 (1965)

Molecular orbital (MO) collision theory

$v_c << v_e$, the electronic motion of the system is expected to adjust adiabatically to the changing position of colliding nuclei.

→ The transient formation of molecular orbitals (MO's)

MO's can connect different shells. An electron occupies a MO and become excited during the collision to a higher energy at smaller separation. It contains vacancies after the collision.

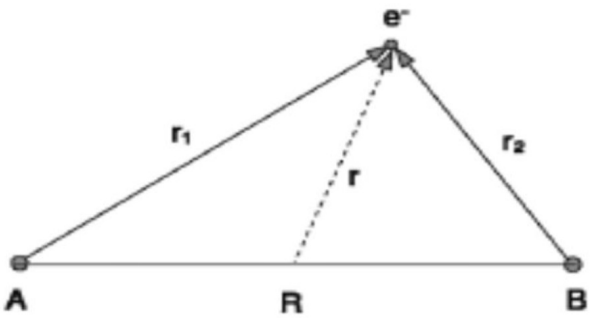

Coordinate system for a quasimolecule composed of an electron e^- and two nuclei *A* and *B*.

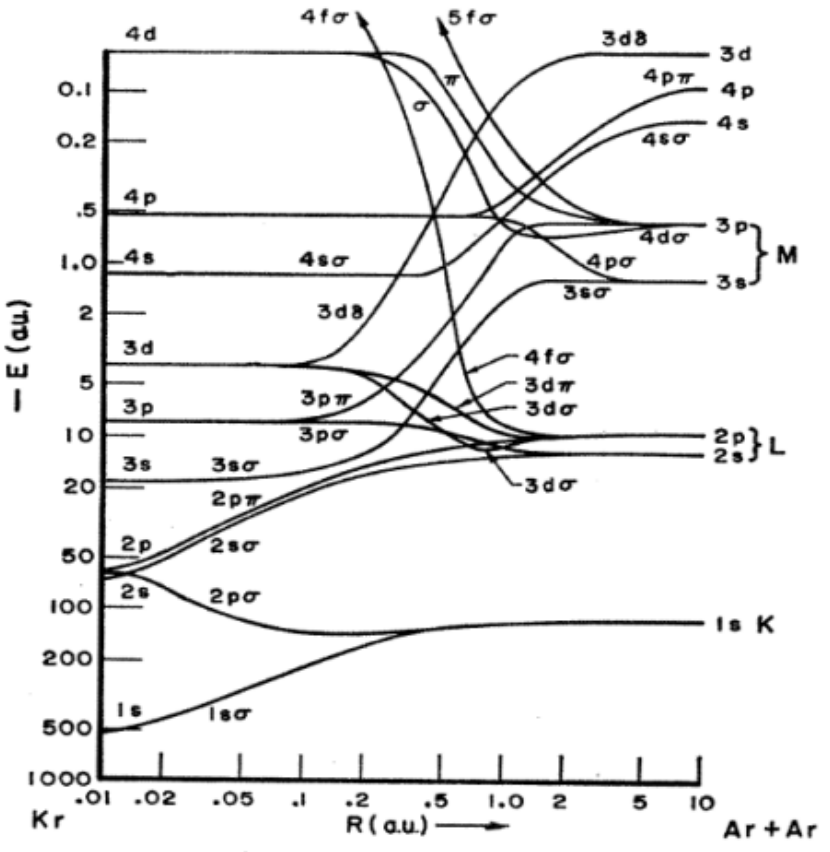

Energy levels of diabatic (H_2^+-like) molecular orbitals of the Ar-Ar system.

J. Eichler, Lectures on ion-atom collisions

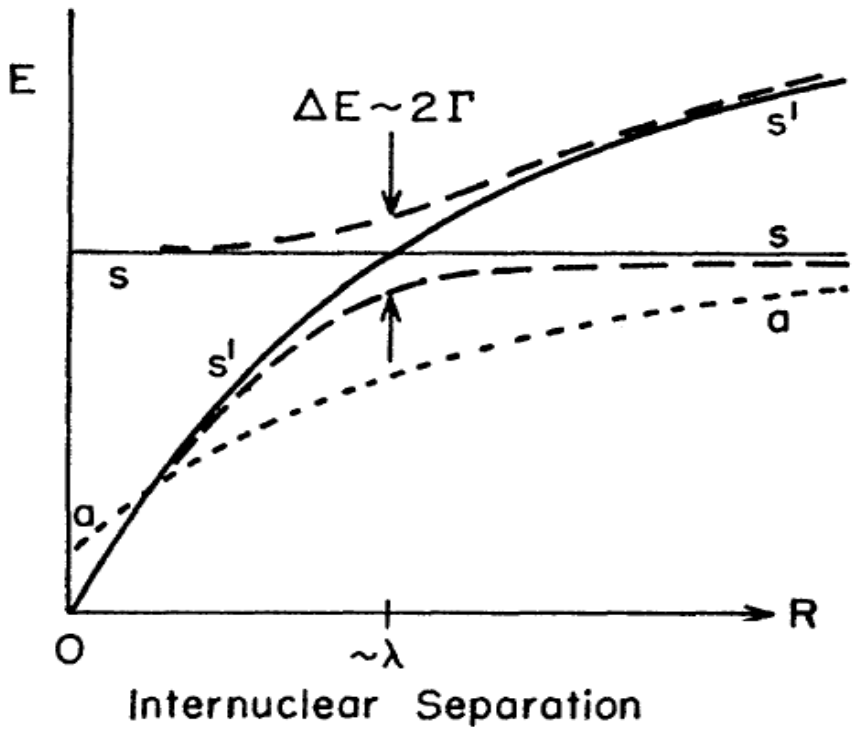

FIG. 2. Crossing of potential curves. Two potential curves for the states s' and s may cross in a certain approximation (such as in a single configuration molecular orbital theory). In a higher approximation, the curves repel each other. If the atoms approach each other slowly in state s, an adiabatic transition from s to s' will occur. If they approach each other rapidly, a diabatic transition from s to s will occur.

W. Lichten, PR 131 (1963)

Nuclear quenching factor

q_{nc} = η/ε ratio

Some puts:

$$q_{nc}(\varepsilon) = \frac{\varepsilon \cdot S_{el}(\varepsilon)}{S_{nc}(\varepsilon) + S_{el}(\varepsilon)}$$

RHS: integrated value
LHS: differential value

and insight. The voluminous literature that has accumulated since then attests to the unfortunate fact that experimental determination of W is often very easy, but *accurate* determination is not. This literature abounds in disparities and contradictions, and even the greatly augmented activity of the past decade has failed to resolve many of them. It is a pity that published tables of experimental data do not bear a symbol indicating whether or not the data are correct.

R. L. PLATZMAN International Journal of Applied Radiation and Isotopes, 1961, Vol. 10, pp. 116–127.

Wave optics using ultrasound

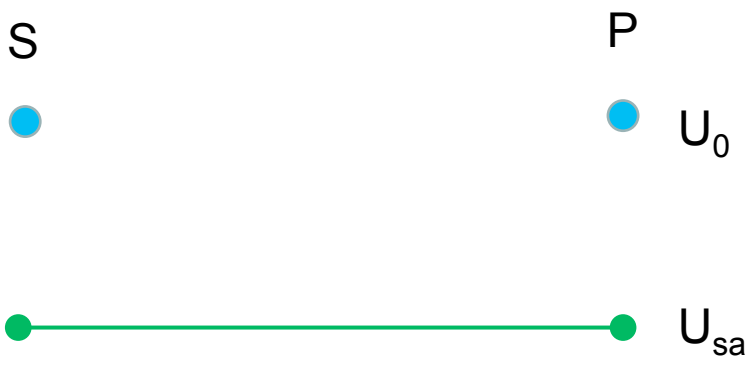

The wave U_0 observed without deflecting object delays $\pi/2$ in phase compared to the wave U_{sa} passing on the central axis.

Hitachi&Takata, Am J Phys 78, 678 (2010).
Hitachi, J Acoust Soc Am, 131, 2463 (2011).
Books by
Born&wolf, Jenkins&White, etc.